International Journal of Engineering, Mathematical and Physical Sciences
ISSN: 2517-9934
Vol:10, No:2, 2016

Highly Conductive Polycrystalline Metallic Ring in a Magnetic Field

Isao Tomita

Abstract—Electrical conduction in a quasi-one-dimensional polycrystalline metallic ring with a long electron phase coherence length realized at low temperature is investigated. In this situation, the wave nature of electrons is important in the ring, where the electrical current I can be induced by a vector potential that arises from a static magnetic field applied perpendicularly to the ring's area. It is shown that if the average grain size of the polycrystalline ring becomes large (or comparable to the Fermi wavelength), the electrical current I increases to $\sim I_0$, where I_0 is a current in a disorder-free ring. The cause of this increasing effect is examined, and this takes place if the electron localization length in the polycrystalline potential increases with increasing grain size, which gives rise to coherent connection of tails of a localized electron wave function in the ring and thus provides highly coherent electrical conduction.

Keywords—Electrical Conduction, Electron Phase Coherence, Polycrystalline Metal, Magnetic Field.

I. Introduction

IT is well known that an electric current is induced in a macroscopic metallic ring when a magnetic field $\boldsymbol{B}$ applied to the ring's area increases or decreases in time t. This is derived from Faraday's law of induction: $\mathcal{E} = -d\phi/dt$, where $\mathcal{E}$ is the electromotive force through the wire of the ring and $\phi = |\boldsymbol{B}|S$ is the applied magnetic flux with a ring's area of S. In the case of a static magnetic field, such a current is not induced in the ring because of $\mathcal{E} = 0$. However, if the ring is downsized to that in a mesoscopic scale, where the quantum coherence of an electron is preserved, a current can be induced by a vector potential $\boldsymbol{A}$ that arises from a static magnetic field $\boldsymbol{B} = \boldsymbol{\nabla} \times \boldsymbol{A}$ [1]–[3]. Here, to preserve its quantum coherence, the circumference of the ring should be smaller than the phase coherence length (or the inelastic scattering length) l_ϕ, which is the length that an electron does not change the size of its energy and momentum before scattering with electrons and phonons. This l_ϕ is about $10\,\mu$m in metals at a temperature of ~ 0.1 K. Even at this temperature, some metals (e.g., Au, Cu) are not superconductors because of very weak electron-phonon coupling, and these kinds of metals are dealt with in this paper.

The reason why the current is induced by the vector potential is that it yields the asymmetry of electron momentum distribution because the electron momentum $\pm\boldsymbol{p}$ is changed as $\pm\boldsymbol{p} - e\boldsymbol{A}$ with the vector potential $\boldsymbol{A}$ [4]. Here, the plus (minus) sign of $\boldsymbol{p}$ denotes clockwise (counterclockwise) propagation of electrons in the ring and e is the electric charge. This asymmetric momentum distribution produces a finite current in one direction of the ring after statistical averaging.

Isao Tomita is with Department of Electrical and Computer Engineering, National Institute of Technology, Gifu College, 2236-2 Kamimakuwa, Motosu, Gifu 501-0495, Japan and with School of Engineering, University of Glasgow, Glasgow G12 8QQ, United Kingdom (e-mail: itomita@gifu-nct.ac.jp).

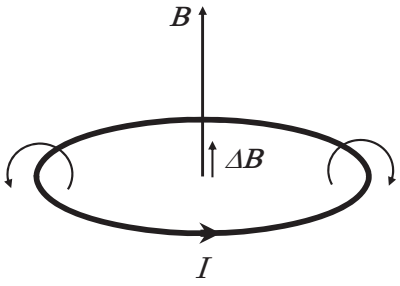

Fig. 1 The presence of an additional magnetic field $\Delta\boldsymbol{B}$ to a static magnetic field $\boldsymbol{B}$. A current I in the ring is generated from the original $\boldsymbol{B}$. $\Delta\boldsymbol{B}$ is produced from I via Ampere's law.

Recent microfabrication technology has enabled producing such a mesoscopic ring, and experiments to detect such a current in the ring [5]–[7] have actually shown its presence by measuring a change $\Delta\boldsymbol{B}$ in the magnetic field $\boldsymbol{B}$ with the help of superconducting quantum interference devices (SQUIDs), where $\Delta\boldsymbol{B}$ arises from the presence of the current I via Ampere's law (See Fig. 1).

Some of the experimental results [5], [6] for the current were well explained by theory under situations that fit those in the experiments, but the other [7] remains unexplained. The current in a quasi-one-dimensional gold (Au) ring fabricated on an SiO_2 substrate was much greater than that predicted by theory, where the presence of defects and dislocations in the ring would make the size of the current almost two orders of magnitude smaller than a current I_0 in a disorder-free ring. But, the observed current was on the same order of I_0.

In the next section, we show previous theoretical treatment of the current I in a disordered metallic ring and point out a problem with it.

II. Theory and Its Problem

To calculate the current, we use the following Hamiltonian $\mathcal{H}$ for the electrons in a quasi-one-dimensional ring with a static magnetic field $\boldsymbol{B}(\boldsymbol{r}) = \boldsymbol{\nabla} \times \boldsymbol{A}(\boldsymbol{r})$ applied in the perpendicular direction to the ring's area [8].

$$\begin{aligned} \mathcal{H} &= \frac{1}{2m}\left(\frac{\hbar}{i}\boldsymbol{\nabla} - e\boldsymbol{A}(\boldsymbol{r})\right)^2 + V(\boldsymbol{r}) \\ &= \frac{1}{2m}\left(\frac{\hbar}{i}\boldsymbol{\nabla} - \frac{2\pi\hbar}{L_x}\frac{\phi}{\phi_0}\boldsymbol{e}_x\right)^2 + V(\boldsymbol{r}), \end{aligned} \tag{1}$$

where $\boldsymbol{r} = (x, y, z)$, the x direction is taken along the wire of the ring with a length of L_x, the y and z directions are taken vertically to it with a wire cross-section of $L_y \times L_z$ ($L_y, L_z \ll L_x$), $\boldsymbol{e}_x$ is the unit vector in the x direction, m is the electron

mass, $\hbar$ is the Planck's constant h divided by 2π, $\phi = |\boldsymbol{B}|S$ is a magnetic flux with S being the ring's area, and $\phi_0 = h/e$. $V(\boldsymbol{r})$ is a disordered potential for defects and dislocations, which is defined by

$$V(\boldsymbol{r}) = \sum_{i=1}^{N} v_i\, \delta(\boldsymbol{r} - \boldsymbol{R}_i), \tag{2}$$

where $\boldsymbol{R}_i\,(i = 1, 2, ..., N)$ and v_i are the i-th position and strength of the disorder, respectively, and the statistics of the disordered potential is of the form

$$\begin{aligned} \big\langle V(\boldsymbol{r})\big\rangle &= 0, & (3)\\ \big\langle V(\boldsymbol{r})V(\boldsymbol{r}')\big\rangle &= \gamma\,\delta(\boldsymbol{r} - \boldsymbol{r}'), & (4)\end{aligned}$$

where γ is a constant and $\big\langle\cdots\big\rangle$ denotes disorder averaging. In the above, the electrons are dealt with as quasi-particles that behave as free particles, where the electron-electron (e-e) interaction is renormalized as the electron mass [9].

The current I in the ring is then calculated as

$$I = \frac{1}{\beta}\sum_{\omega_n} e^{i\omega_n\eta}\sum_{\mathbf{k}} I(k_x)\,\mathcal{G}(\boldsymbol{k},\omega_n) \quad (\eta\to 0_+), \tag{5}$$

where β is the inverse temperature $\beta = 1/T$ in units of $k_{\rm B} = 1$, ω_n is the Matsubara frequency $\omega_n = (2n+1)\pi/\beta$ [10] in units of $\hbar = 1$, $I(k_x) = e\hbar k_x/mL_x$ gives the current vertex, and $\mathcal{G}(\boldsymbol{k},\omega_n)$ is the thermal Green function [11] for a particular disorder configuration with a frequency of ω_n and a wave vector of $\boldsymbol{k} = (k_x, k_y, k_z) = ((2\pi/L_x)\,(n_x - \phi/\phi_0), (2\pi/L_y)\,n_y,\ (2\pi/L_z)\,n_z)\ \ (n_x, n_y, n_z = 0, \pm1, \pm2, ...)$.

In what follows, we calculate a typical current

$$I_{\rm typ} \equiv \big\langle I^2\big\rangle^{\frac{1}{2}} = \Big(\big\langle I\big\rangle^2 + (\Delta I)^2\Big)^{\frac{1}{2}} \tag{6}$$

that includes the fluctuation term ΔI of the current arising from the electron scattering with disorder [12]–[14]. To do this, squaring (5) and taking its disorder averaging, we obtain

$$\begin{aligned}\big\langle I^2\big\rangle &= \frac{1}{\beta^2}\sum_{\omega_n,\zeta_l} e^{i\omega_n\eta}e^{i\zeta_l\eta'}\sum_{\mathbf{k},\mathbf{k}'} I(k_x)I(k_x')\\ &\quad\times\big\langle\mathcal{G}(\boldsymbol{k},\omega_n)\mathcal{G}(\boldsymbol{k}',\zeta_l)\big\rangle\ \ (\eta,\eta'\to 0_+). \qquad (7)\end{aligned}$$

Using the perturbative expansion of $\mathcal{G}(\boldsymbol{k},\omega_n)$ for a weak disordered potential and taking the diagrams of the leading order, as shown in Fig. 2, we can rewrite (7) as

$$\begin{aligned}\big\langle I^2\big\rangle &= \frac{1}{\beta^2}\sum_{\omega_n,\zeta_l} e^{i\omega_n\eta}e^{i\zeta_l\eta'}\sum_{\mathbf{k},\mathbf{p}}\sum_{\mathbf{q}}\\ &\times \Big(I(-k_x+q_{x+})I(k_x)G^2(-\boldsymbol{k}+\boldsymbol{q}_+,\omega_n)\\ &\times G^2(\boldsymbol{k},\zeta_l)K(\boldsymbol{q}_+,\omega_n-\zeta_l) + I(k_x+q_{x-})I(k_x)\\ &\times G^2(\boldsymbol{k}+\boldsymbol{q}_-,\omega_n)G^2(\boldsymbol{k},\zeta_l)D(\boldsymbol{q}_-,\omega_n-\zeta_l)\\ &+ I(-k_x+q_{x+})I(p_x)G^2(-\boldsymbol{k}+\boldsymbol{q}_+,\omega_n)G(\boldsymbol{k},\zeta_l)\\ &\times G(-\boldsymbol{p}+\boldsymbol{q}_+,\omega_n)G^2(\boldsymbol{p},\zeta_l)K^2(\boldsymbol{q}_+,\omega_n-\zeta_l)\\ &+ I(k_x+q_{x-})I(p_x)G^2(\boldsymbol{k}+\boldsymbol{q}_-,\omega_n)G(\boldsymbol{k},\zeta_l)\\ &\times G(\boldsymbol{p}+\boldsymbol{q}_-,\omega_n)G^2(\boldsymbol{p},\zeta_l)D^2(\boldsymbol{q}_-,\omega_n-\zeta_l)\Big), \qquad (8)\end{aligned}$$

where $G = \big\langle\mathcal{G}\big\rangle$ is the disorder-averaged thermal Green function, and K and D are the two-body Green functions, called Cooperon and Diffuson respectively, which are yielded from the cross terms of the expanded Green functions. Note that $\sum_{\mathbf{q}}$ in (8) denotes $\sum_{\mathbf{q}_+}$ for a function of $\boldsymbol{q}_+$ and $\sum_{\mathbf{q}_-}$ for a function of $\boldsymbol{q}_-$.

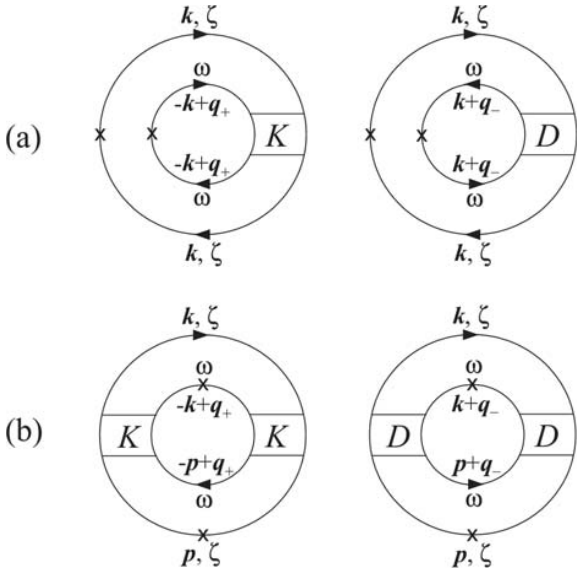

Fig. 2 (a) One-Cooperon and one-Diffuson processes and (b) two-Cooperon and two-Diffuson processes. They contribute to the current as the leading order. The crosses represent the current vertices.

The explicit expressions of G, K, and D are as follows:

$$\begin{aligned} G(\boldsymbol{k},\omega) &= \frac{1}{i\omega - \xi(\boldsymbol{k}) + \frac{i}{2\tau_{\rm e}}\mathrm{sgn}\,\omega}, & (9)\\ K(\boldsymbol{q}_+,\omega-\zeta) &= \frac{1}{2\pi N(0)\tau_{\rm e}^2}\frac{\theta(-\omega\zeta)}{|\omega-\zeta| + D_0|\boldsymbol{q}_+|^2}, & (10)\\ D(\boldsymbol{q}_-,\omega-\zeta) &= \frac{1}{2\pi N(0)\tau_{\rm e}^2}\frac{\theta(-\omega\zeta)}{|\omega-\zeta| + D_0|\boldsymbol{q}_-|^2}, & (11)\end{aligned}$$

where $\xi(\boldsymbol{k}) = E_{\mathbf{k}} - \mu$ with $E_{\mathbf{k}}$ being the electron energy and μ being the chemical potential, $N(0)$ is the density of states, $\tau_{\rm e}$ is the electron elastic scattering time, D_0 is the diffusion constant, and $\theta(x) = 0\,(x\le 0), 1\,(x>0)$.

Making further calculations by substituting (9), (10), and (11) for (8), we obtain

$$\begin{aligned}\big\langle I^2(T)\big\rangle &= \sum_{n=1}^{\infty} g\left(\frac{n^2T}{E_{\rm c}}\right)\big\langle I_n^2(T=0)\big\rangle\\ &\quad\times\sin^2\left(2\pi n\frac{\phi}{\phi_0}\right), \qquad (12)\end{aligned}$$

where $E_{\rm c} = (\pi/2)(hD_0/L_x^2)$, $g(x)$ gives a temperature dependence and is defined by

$$g(x) = \frac{\pi^6}{3}x^2\sum_{n=1}^{\infty} n\,\exp\left(-\sqrt{2\pi^3 nx}\right) \tag{13}$$

and $\big\langle I_n^2(T=0)\big\rangle$ takes the form

$$\big\langle I_n^2(T=0)\big\rangle = \frac{8}{3\pi^2 n^3}\left(\frac{l_{\rm e}}{L_x}\right)^2 I_0^2, \tag{14}$$

where l_e is the electron elastic scattering length that is defined by $l_e = v_F \tau_e$ with the Fermi velocity v_F.

From (14), we can see that the first term with $n = 1$ is the largest component in $\langle I_n^2 \rangle$ because the other terms drop off as n^{-3}. In addition, we can see from (12) that the largest component $\langle I_1^2 \rangle^{1/2}$ has a flux dependence of ϕ_0. This agrees well with the experimental result (See Fig. 2 (d) in [7]).

The temperature dependence $g^{1/2}(T/E_c)$ obtained from (13) for the first-harmonic ($n = 1$) current is also in good agreement with that measured in the experiment, as depicted in Fig. 3 (See also Fig. 3 (a) in [7]).

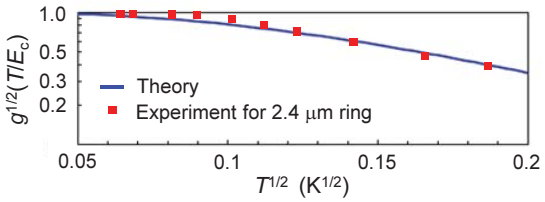

Fig. 3 Comparison between theoretical and experimental temperature dependences. The blue curve is $g^{1/2}(T/E_c)$ calculated from (13) for a 2.4 μm ring, and the red squares are the experimental data measured for the same-sized ring [7], excluding data for a 1.4 μm × 2.6 μm loop.

Although the theoretical flux and temperature dependences agree well with the experimental data, the size of the current for the first harmonic

$$\langle I_1^2 \rangle^{\frac{1}{2}} = 2\sqrt{\frac{8}{3\pi^2}} \frac{l_e}{L_x} I_0 \approx 1.04 \frac{l_e}{L_x} I_0, \qquad (15)$$

does not match the measured value $\sim I_0$ because l_e/L_x has a size of $\sim 1/100$. In (15), a factor 2 in front of the square root comes from spin multiplicity of electrons.

To solve the problem with the discrepancy between the theoretical and experimental values, some new ideas containing the effect of the e-e interaction [15]–[17] have been proposed. But, the discrepancy has not yet been resolved. As a matter of fact, the effect of the e-e interaction works to reduce the size of the current, and the reduction size becomes large as the strength of the e-e interaction increases. For this reason, other possibilities than this should be searched in order to explain the cause of the large current.

III. Solution of Problem and Discussion

In this section, we reconsider whether the model disordered potential was appropriate or not as one of the possibilities.

In the experiment [7], the Au ring was fabricated from an Au film formed on an amorphous SiO_2 substrate by deposition of Au vapor on the substrate. In this case, the experiment [7] did not point it out, but it is known that polycrystalline Au is formed on it [18]. In most theories, the correlation function of the disordered potential is assumed to be of the form $\langle V(\boldsymbol{r})V(\boldsymbol{r}')\rangle = \gamma\,\delta(\boldsymbol{r}-\boldsymbol{r}')$ for analytical calculations (or $\langle V_n V_{n'}\rangle = \gamma\,\delta_{n,n'}$ for numerical calculations) because it makes the calculations easier, where the effective range of the disorder is very short compared with the Fermi wavelength. However, this assumption has no basis.

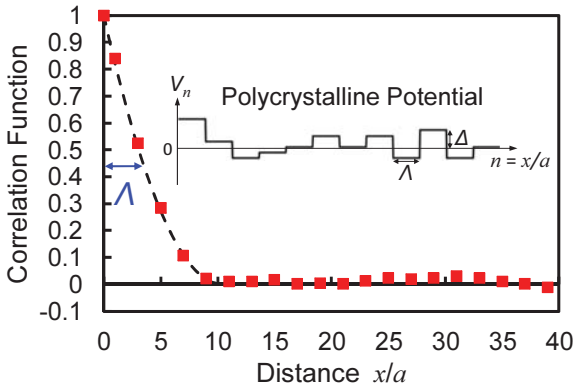

Fig. 4 Correlation function of a polycrystalline potential. The inset shows the polycrystalline potential with an average potential height Δ and an average grain size Λ (a is the atomic distance). The red squares are computer-generated points for the disorder-averaged correlation function.

The correlation function of the disordered potential in the Au ring on the amorphous SiO_2 substrate would be different from the above short-ranged type, and a correlation length (or grain size) that is large compared with the Fermi wavelength would be possible. This would considerably affect the size of the current.

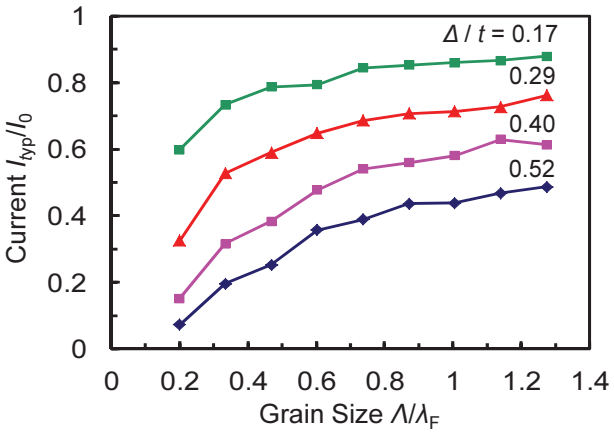

Fig. 5 Dependence of the current I_{typ} on the average grain size Λ, where I_{typ} and Λ are normalized by a current I_0 in a disorder-free ring and the Fermi wavelength λ_F, respectively, t is the electron hopping matrix element that corresponds to the electron kinetic energy, and the average potential height Δ is taken as $0.17t$, $0.29t$, $0.40t$, $0.52t$.

Motivated by that possibility, some theoretical studies [19]–[21] have been made to disclose the effect of a finite grain size in polycrystalline Au on the current; more specifically, if we use a correlation function with an average grain size Λ and an average potential height Δ, as shown in Fig. 4 [20], the current can be increased to $\sim I_0$ as the average grain size Λ becomes large (or comparable to the Fermi wavelength λ_F), as depicted in Fig. 5. Here, the increasing rate (e.g., the ratio of I_{typ} between $\Lambda = 1.3\lambda_F$ and $0.2\lambda_F$) becomes higher for larger potential heights.

The above results were surmised to be due to the relaxation of electron localization, but this has not yet been proved. To

do this, we examine it via a theory developed by Anderson *et al.* [22] used for the analysis of the conductance in a one-dimensional disordered wire with quantum coherence. This theory relates the conductance g of the disordered wire with a length of L to the electron localization length ξ as

$$g = \kappa\, e^{-\frac{L}{\xi}}, \tag{16}$$

where κ is a constant. If the wire is ring-shaped, L is the perimeter of the ring (i.e., $L = L_x$). Since the current I is proportional to the conductance g, (16) can be rewritten as

$$I = C\, e^{-\frac{L}{\xi}}, \tag{17}$$

where C is a constant. This is interpreted as follows: If an electron is localized at the center of the disordered wire with $L(> \xi)$, the tail of the wave function near both ends of the wire is $\psi \sim e^{-L/2\xi}$. Thus the quantum link between both ends is very weak. In this case, the probability that an electron at one end comes to the other end is in proportion to $|\psi|^2 \sim e^{-L/\xi}$, which gives the transmission probability to which the current is proportional. On the other hand, the relation between the average grain size Λ and the localization length ξ is given as

$$\xi = b\,\Lambda, \tag{18}$$

where b is a constant. This is because the increasing rate of ξ is the same as that of Λ, which is obtained from the scale transformation for the polycrystalline potential, as shown in Fig. 6.

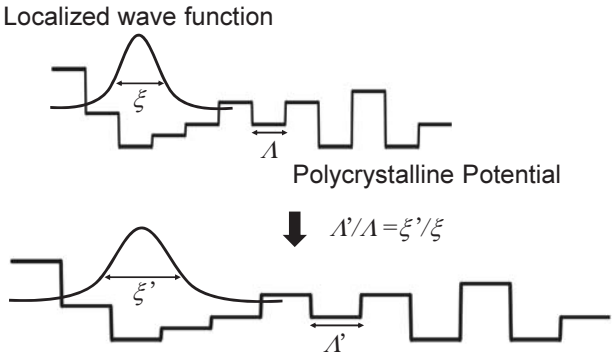

Fig. 6 Relation between the average grain size Λ and the localization length ξ when the scale transformation of the polycrystalline potential is performed, which gives proportionality between Λ and ξ.

Substituting (18) for (17), we obtain

$$I = C\, e^{-\alpha \frac{L}{\Lambda}}, \tag{19}$$

where $\alpha = 1/b$. In Fig. 7, we plot the normalized current I/C as a function of the average grain size Λ normalized by the Fermi wavelength $\lambda_{\rm F}$, where the parameter α is set as $\alpha = \eta\lambda_{\rm F}/L$ $(\eta = 0.12, 0.27, 0.53, 0.87)$.

Comparing the curves in Figs. 5 and 7, we can see that they show a very similar behavior, and we can conclude that the enhanced current with the increased grain size is caused by the extended localization length. There are some deviations in the curves between Figs. 5 and 7, but these will be improved if the analysis in Fig. 7 takes account of the omitted fluctuation term ΔI, as seen in (6).

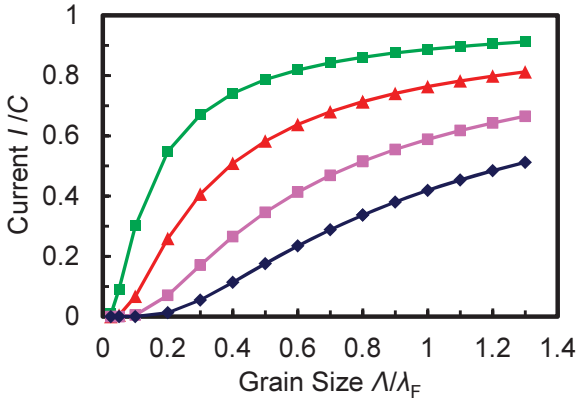

Fig. 7 Dependence of the current $I = C\, e^{-\alpha L/\Lambda}$ on the grain size Λ, where α is set as $\alpha = \eta\lambda_{\rm F}/L$ $(\eta = 0.12, 0.27, 0.53, 0.87)$, and I and Λ are normalized by the constant C and the Fermi wavelength $\lambda_{\rm F}$, respectively.

IV. Summary

We have investigated the electrical conduction in a quasi-one-dimensional polycrystalline metallic ring formed on an amorphous SiO_2 substrate in the region where the wave nature of electrons is important. If we calculate the current with a short-ranged disordered potential, we have had a disagreement in size with the current measured in the experiment ($\sim I_0$). Thus, recalculating the current by taking into consideration the actual metallic state (or the polycrystalline state), we have obtained an increased current on the order of I_0. To disclose this increasing mechanism, we have performed an analysis using an electrical conduction theory developed by Anderson *et al.* [22] while taking account of an increased electron localization length due to an enlarged grain size, which is obtained from the scale transformation. From this analysis, we have observed a very similar behavior for the recalculated current and thus have concluded that high electrical conduction in the polycrystalline ring is caused by the increased localization length due to the enlarged grain size.

Acknowledgment

The author would like to thank National Institute of Technology, Gifu College and Institute of National Colleges of Technology of Japan for the financial support.

References

[1] M. Büttiker, Y. Imry, and R. Landauer, "Josephson behavior in small normal one-dimensional rings," Phys. Lett. 96A, 1983, pp.365-367.
[2] Y. Imry and N. S. Shiren, "Energy averaging and the flux-periodic phenomena in small normal-metal rings," Phys. Rev. B 33, 1986, pp.7992-7997.
[3] N. Trivedi and D. A. Browne, "Mesoscopic ring in a magnetic field: Reactive and dissipative response," Phys. Rev. B 38, 1988, pp. 9581-9593.
[4] J. J. Sakurai, Modern Quantum Mechanics, Revised ed., New York: Addison-Wesley Publishing, 1994. Chap. 2.
[5] L. P. Levy, G. Dolan J. Dunsmuir, and H. Bouchiat, "Magnetization of mesoscopic copper rings: Evidence for persistent currents," Phys. Rev. Lett. 64, 1990, pp. 2074-2077.
[6] D. Mailly, C. Chapelier, and A. Benoit, "Experimental observation of persistent currents in GaAs-AlGaAs single loop," Phys. Rev. Lett. 70, 1993, pp. 2020-2023.

[7] V. Chandrasekhar, R. A. Webb, M. J. Brady, M. B. Ketchen, W. J. Gallagher, and A. Kleinsasser, "Magnetic response of a single, isolated gold loop," Phys. Rev. Lett. 67, 1991, pp. 3578-3581.
[8] E. K. Riedel and F. von Oppen, "Mesoscopic persistent current in small rings," Phys. Rev. B 47, 1993, pp. 15449-15459.
[9] P. Nozieres and D. Pines, The Theory of Quantum Liquids, Vol. 1, 1st ed., New York: Benjamin, 1966. Chap. 1.
[10] T. Matsubara, "A new approach to quantum-statistical mechanics," Prog. Theor. Phys. 14, 1955, pp. 351-378.
[11] A. A. Abrikosov, L. P. Gorkov, and I. E. Dzyaloshinski, Methods of Quantum Field Theory in Statistical Physics, 1st ed., New York: Dover, 1975.
[12] S. Washburn and R. A. Webb, "Aharonov-Bohm effect in normal metal quantum coherence and transport," Adv. Phys. 35, 1986, pp.375-422. This paper reports that the measurement of a conductance through an Au wire or ring at very low temperature (< 1 K) showed a large conductance fluctuation arising from the electron scattering with disorder in addition to the average conductance. This also holds in measuring a current at very low temperature.
[13] A. D. Stone, "Magnetoresistance fluctuations in mesoscopic wires and rings," Phys. Rev. Lett. 54, 1985, pp.2692-2695.
[14] P. A. Lee and A. D. Stone, "Universal conductance fluctuations in metals," Phys. Rev. Lett. 55, 1985, pp.1622-1625.
[15] G. Bouzerar, D. Poilblanc, and G. Montambaux, "Persistent currents in one-dimensional disordered rings of interacting electrons," Phys. Rev. B 49, 1994, pp. 8258-8262.
[16] H. Kato H and D. Yoshioka, "Suppression of persistent currents in one-dimensional disordered rings by the Coulomb interaction," Phys. Rev. B 50, 1994, pp. 4943-4946.
[17] D. Yoshioka and H. Kato, "The effect of the Coulomb interaction on the mesoscopic persistent current," Physica B 212, 1995, pp. 251-255. The Hartree and Fock terms in this paper seemingly give an enhancement in the current, but actually the Fock term has a different sign from the Hartree term, so they almost cancel each other in summation, and eventually the e-e interaction does not contribute to an increase in the current.
[18] P. M. Th. M. van Attekum, P. H. Woerlee, G. C. Verkade, and A. A. M. Hoeben, "Influence of grain boundaries and surface Debye temperature on the electrical resistance of thin gold films," Phys. Rev. B 29, 1984, pp. 645-650.
[19] X. Chen, Z. Y. Deng, W. Lu, and S. C. Shen, "Persistent current in a one-dimensional correlated disordered ring," Phys. Rev. B 61, 2000, pp. 2008-2013.
[20] I. Tomita, "Persistent current in a one-dimensional correlated disordered ring," Physica A 308, 2002, pp. 1-14.
[21] Y. M. Liu, R. W. Peng, X. Q. Huang, M. Wang, A. Hu, and S. S. Jiang, "Absence of suppression in the persistent current by delocalization in random-dimer mesoscopic rings," J. Phys. Soc. Japan 72, 2003, pp. 346-351.
[22] P. W. Anderson, D. J. Thouless, E. Abrahams, and D. S. Fisher, "New method for a scaling theory of localization," Phys. Rev. B 22, 1980, pp.3519-3526.